Journal of Materials, Processing and Design (2023)
Clausius Scientific Press, Canada

DOI: 10.23977/jmpd.2023.070303
ISSN 2516-0923 Vol. 7 Num. 3

Alumina-based crucibles with enhanced thermal shock resistance via reinforcement of mullite fibers

Hongna Fan[1,*], Jiaxian Fan[2], Xin Li[1], Changjian Qi[1], Weiwei Han[1], Xiqing Xu[2]

[1]AECC Aegis Advanced Protective Technology Co., Ltd, Tianjin, 300399, China
[2]School of Materials Science & Engineering, Chang'an University, Xi'an, 710061, China
[*]Corresponding author

Keywords: Alumina-based crucible, superalloy smelting, thermal shock resistance, mullite fiber, mechanical property

Abstract: Crucible is the indispensable vessel in smelting of superalloy, and the service life of crucibles is quite important to the development of superalloy. In order to extend the service life of crucible for superalloy smelting, alumina-based crucibles are prepared by slip casting, and mullite fibers are used as reinforcement phase. The effect of mullite fibers on the microstructure and property of the crucibles was studied. The appropriate content of mullite fibers are beneficial to the comprehensive performance of the crucibles. The reinforcement mechanism of mullite fibers includes crack deflection, fiber extraction, and fiber bridging, through which fibers hinder the initiation and propagation of cracks in ceramics. For the crucible samples with 3 wt% of mullite fibers, the values of flexure strength are 22.47 MPa and 19.14 MPa at room temperature and high-temperature, respectively. After thermal shock for 5 times, the residual room-temperature flexural strength is 16.65 MPa and the strength retention rate is 74.1%. It is confirmed that, the 3 wt% of mullite fibers improves the thermal shock resistance of the crucible, which is beneficial for extending the service life of the crucible for superalloy melting.

1. Introduction

Superalloy [1-3] is a class of metal material that has excellent performance at high temperature. Superalloys generally display superior high-temperature strength, resistance to oxidation, and resistance to thermal corrosion, as well as excellent fatigue performance, fracture toughness and other comprehensive properties. Superalloys are widely employed in the aviation jet engines and various industrial gas turbines [4,5]. The preparation of superalloy has a significant impact on their properties. In order to obtain superalloy meeting the usage conditions along with excellent performance, it is necessary to pay attention to the melting and preparation process of the alloys. At present, the main method for preparing most superalloys is vacuum induction melting [6,7]. Crucibles [8-10] are employed as the container for vacuum induction melting, and their performance and quality are very important for the preparation of superalloys.

The crucibles are faced with high temperatures of 1550℃ during melting of superalloy; therefore, high temperature resistance is demanded. Meanwhile, under the environments of high temperature and vacuum during melting of superalloys, the crucible and superalloy are faced with great

challenges in temperature and pressure, and various physical and chemical interactions occur between the crucible and alloy melts, which inevitably leads to corrosion of the crucible material and contamination of the melt. Therefore, good chemical stability [11-13] is required for the crucible. Moreover, the crucible needs to withstand extremely high temperatures during the melting process and cools down quickly during the casting process. The rapid periodical heating and cooling effects easily result in stress of expansion and contraction within the crucible, which leads to significant decrease in strength, surface peeling and even fracture. Therefore, it is required that the crucible have excellent thermal shock resistance [14-18]. A crucible with excellent thermal shock resistance is beneficial to avoid pollution caused by the detachment of crucible materials, improve the performance of high-temperature alloys, and greatly reduce production costs. Therefore, investigation on alumina crucibles with good thermal shock resistance for melting and extending the working life of the crucibles is of great significance for the development of high-temperature alloy melting.

MgO, CaO and Al_2O_3 are common crucible materials for melting of superalloy, which have high melting point, chemical stability with superalloy melts, and resistance to high temperatures above 1550℃ [19, 20]. However, under high temperature and vacuum conditions, MgO crucibles generally supply oxygen to the alloy, while CaO crucibles are prone to hydration. In contrast, Al_2O_3 ceramics have good oxidation resistance, chemical stability, high temperature resistance, and high-temperature strength; moreover, they are abundant in resources and low in price, making them the most widely used oxide ceramics [21-26]. At present, commonly used alumina crucibles have poor thermal shock resistance, the surface of the crucible often cracks and falls after once usage, making the continue use impossible. The short service life increases the production cost of high-temperature alloys.

To improve the mechanical property and thermal shock resistance of ceramics, various investigations are performed, among which ceramics reinforced by distribution of fibers or whiskers are widely reported [27-30], displaying superior properties compared to the matrix material. Mullite fiber, known as a superior refractory material, has superior resistance to thermal shock, strong resistance to creep deformation, and high load softening temperature [31-33], which can have significant effects on the high-temperature properties of silica-based ceramic cores. Mullite is a very important composition in Al_2O_3-SiO_2 system and the most stable binary solid solution compound. It has good thermal shock resistance, high temperature creep resistance, stable chemical properties, low coefficient of thermal expansion and thermal conductivity, and is a high-quality high-temperature structural refractory. The introduction of mullite fibers in ceramics is expected to increase the fracture energy, enhance the loss tolerance, strengthen the matrix. However, thermal shock resistance of crucibles enhanced by mullite fibers is seldom reported.

In attempt to improve the high-temperature resistance and thermal shock resistance of crucibles, alumina-based crucibles are prepared by slip casting, and mullite fibers are used as reinforcement phase. The effects of mullite fiber content on the mechanical property and thermal shock resistance are explored, and the mechanisms are analyzed.

2. Materials and methods

2.1. Raw materials

The major raw materials are consisted of two types of Al_2O_3 powders with different particle sizes, and SiO_2 powders with different particle sizes as the auxiliary materials. Mullite fibers are employed as reinforcement phase with mass percent of 0~4%, whose average diameter is about 8 μm, and the average length is above 100 μm. The dimensional features and specific information of the powders and mullite fibers are listed in Table 1. Ammonia solution was used as pH regulator,

and the dispersant is the mixture of triammonium citrate and gum arabic with volume ratio of 1:1.

Table 1: Information of the raw materials

Raw powders	Purity	Average grain size	Mass percent	Production place **1.1.1.1 Production Place** • **1.1.1.2 Production Place** • • **1.1.1.3 Production Place** •
Fine Al_2O_3	>99%	0.3 μm	18.6%	Anhui
Coarse Al_2O_3	>99%	2 μm	41.4%	Henan
Fine SiO_2	>99%	35 μm	10%	Jiangsu
Coarse SiO_2	>99%	320 μm	30%	Jiangsu
Mullite fibers	>95%	D=8 μm, L>100 μm	0~4%	Shandong

2.2. Sample preparation

The raw materials were mixed in deionized water, and the slurry was prepared with solid loading of 66 vol%. In order to avoid agglomeration during the mixing process, water and dispersant were mixed first, after which fine Al_2O_3 was added, and other raw materials were added at last. After ball milling for 2 h using a planetary miller, homogeneous slurry with different content of mullite fibers was obtained. The prepared suspension were poured into a gypsum mold with inner size of 6 mm × 6 mm × 60 mm. After the slurry solidified in the gypsum mold, demoulding was carried out. Then the green bodies are dried at room temperature, and then placed in a drying oven at 60 ℃. The dried bodies were sintered at 1300 ℃ for 2 h to obtain ceramic samples.

2.3. Testing and characterization

Archimedes' method according to ASTM C373 was conducted to determine the bulk density and porosity of the sintered ceramics. Scanning electron microscope (SEM, JSM-5600LV, JEOL, Japan) was employed to analyze the microstructure of the fracture surface. X-ray diffraction analysis (XRD,D/Max-2500v/pc, Rigaku, Japan) with Cu Kα radiation was performed to characterize the phase composition. The length of samples before and after sintering were measured using a vernier scale, to determine the linear shrinkage of samples. The bending strength were tested by universal testing machine (HMOR16-300LX, China) at room temperature and 1540℃. The thermal expansion coefficient of the sintered sample was measured using a thermal expansion instrument (DIL402 PC, NETZSCH, German).

The thermal shock resistance of sintered samples is measured by rapid cooling in air. To evaluate the thermal shock resistance of the material, the sample was heated at 1300℃ for 0.5 h before air cooling and quenching. After cooling in air for 10 min, the sample was further heated at 1300℃ for 0.5 h. The sample underwent repeated cycles of rapid heating and cooling, and the residual strength of the sample after air quenching was measured at different cycles.

3. Results and discussion

3.1. Physical property

The effect of mullite fiber content on the linear shrinkage, apparent porosity, and bulk density of the crucible samples sintered at 1300 ℃ is shown in Figure 1. After fibers are added, the linear shrinkage shows a decreasing trend, which decreases from 1.06% to 0.89% as 1 wt% of mullite fibers are doped. The decreasing trend of linear shrinkage is attributed to the large aspect ratio of mullite fibers, as the fibers form network structures and hinder the structural densification as well as volume shrinkage of ceramics. Due to the hindering of densification by mullite fibers, the content of pores in ceramic samples increases and leading to higher apparent porosity, whose value increases from 18.7% to 24.8% as 1 wt% of mullite fibers are doped. On the contrary, the bulk density decreases from 2.37 g/cm^3 to 2.33 g/cm^3 with the increasing content of fiber from 0 to 1 wt%, attributed to the increase of porosity.

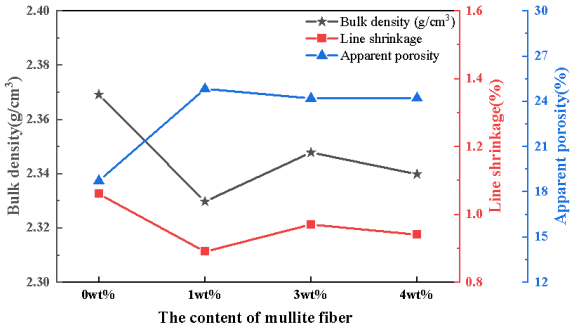

Figure 1: The influence of fiber content on line shrinkage, apparent porosity and bulk density of crucible samples.

As shown in Figure 2, the addition of fibers has a significant impact on the thermal expansion coefficient of ceramics. The thermal expansion coefficient of the crucible samples increases significantly from 2.77×10^{-6} to 6.96×10^{-6} with the increasing content of mullite fibers from 0 to 1 wt%, but the coefficient basically remains unchanged ranging from 6.80×10^{-6} to 6.96×10^{-6} when the fiber content continues to increase to 4 wt%. Thermal expansion is a phenomenon based on the change of average distance between atoms in the lattice structure during the variation of temperature. Due to the different thermal expansion coefficients between mullite fibers and the matrix, thermal stresses are generated between the different phases during heating, and lead to additional expansion. Therefore, the doping of mullite fibers obviously increases the thermal expansion coefficient of crucible samples.

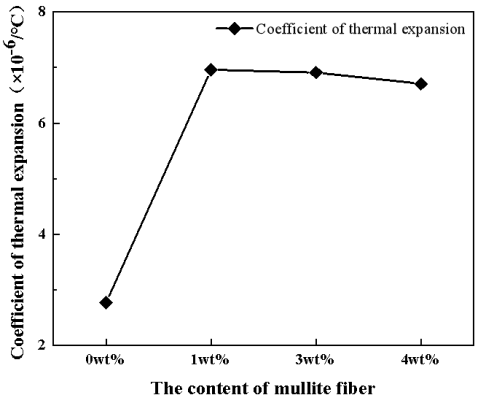

Figure 2: The influence of fiber content on thermal expansion coefficient.

3.2. Flexural strength

Flexural strengths of the crucible sample with different content of mullite fibers are measured at room temperature and high temperature, as shown in Fig. 3. The effect of mullite fiber content on the flexural strength is ascribed to two aspects. On one hand, the volume fraction of pores increases with the doping of mullite fibers, which is not conducive to the mechanical property of ceramics, considering that pores easily turn to the main location for defect formation, where the cracks and other defects first form, leading to decreased strength of ceramics with higher porosity. On the other hand, the fibers can reinforce the flexural strength by fiber extraction, fiber deflection, and fiber bridging. As shown in Fig. 3, with the increase of fiber content, the room temperature and high temperature strength showed a trend of first increasing and then decreasing, suggesting that the deteriorate caused by pores is level-pegging with the reinforcement of fibers. As the weight percent of mullite fibers is 3 wt%, its room flexural strength showed the highest values of 22.47 MPa and 19.14 MPa at temperature and high temperature, respectively.

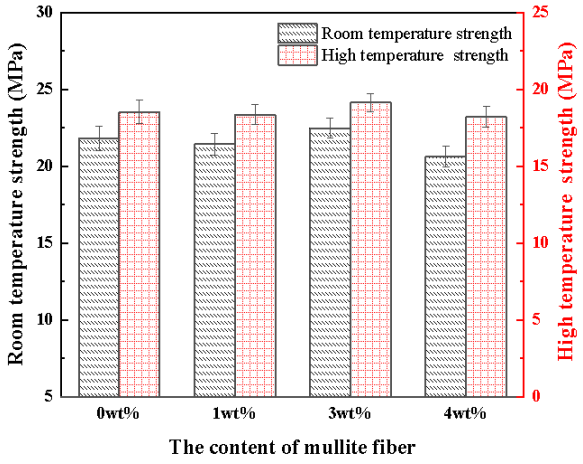

Figure 3: The influence of fiber content on flexural strength at room temperature and high temperature.

3.3. Phase composition and microstructure

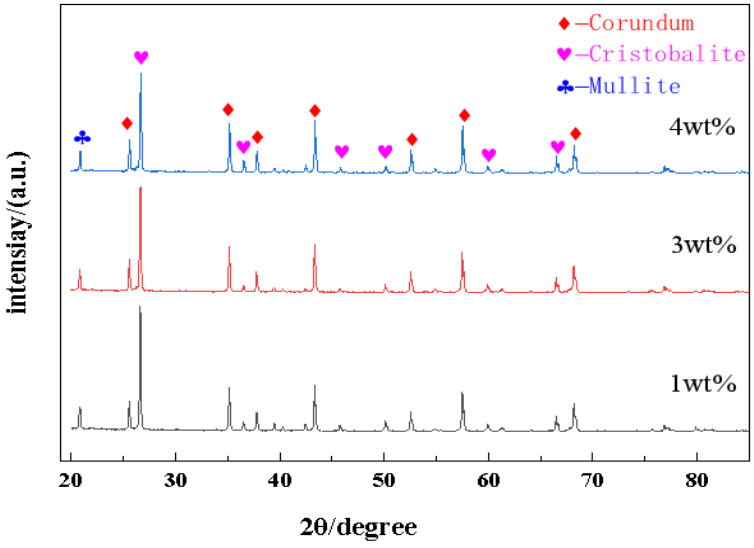

Figure 4: XRD patterns of crucible samples with different contents of mullite fibers

Fig. 4 shows the XRD patterns of crucible samples with different contents of mullite fibers. Apart from the diffraction peaks for corundum, cristobalite and mullite detected in the XRD patterns, no other new phases were visible. It is indicated that, neither other new composition nor impurity elements were introduced into the sample.

SEM images are taken to analyze the fracture morphology of samples with different fiber content, as shown in Fig 5. As the content of mullite fibers is 1 wt%, a small amount of fibers can be observed in the matrix. Due to the low fiber content, fiber extraction and other phenomena can only be detected in local areas. When the content of mullite fibers is 4 wt%, due to the high content of mullite fibers, they aggregate and distributed unevenly in the matrix, which is agreed with the decreased mechanical property. According to the SEM image, it is suggested that crack deflection occurs in the presence of fibers, which reduces the stress field intensity in the material and leads to enhanced flexural strength. Fiber pulling out is also detected in the microstructure, which requires energy consumption, relaxes the stress at the crack tip, reduces the speed of crack propagation, and plays a role in strengthening and toughening. In addition, for fibers with a specific orientation distribution, bridging will occur, connecting the two sides of the crack and applying a certain amount of compressive stress on the surface of the crack. The presence of compressive stress will offset the tensile stress at the crack tip, closing the crack and hindering its further expansion, thus beneficial to the reinforcement effect. The occurrence of these three phenomena contributes to hindering the initiation and propagation of cracks, thereby improving the performance of the crucible, indicating that the addition of an appropriate amount of fibers can play a role of reinforcement.

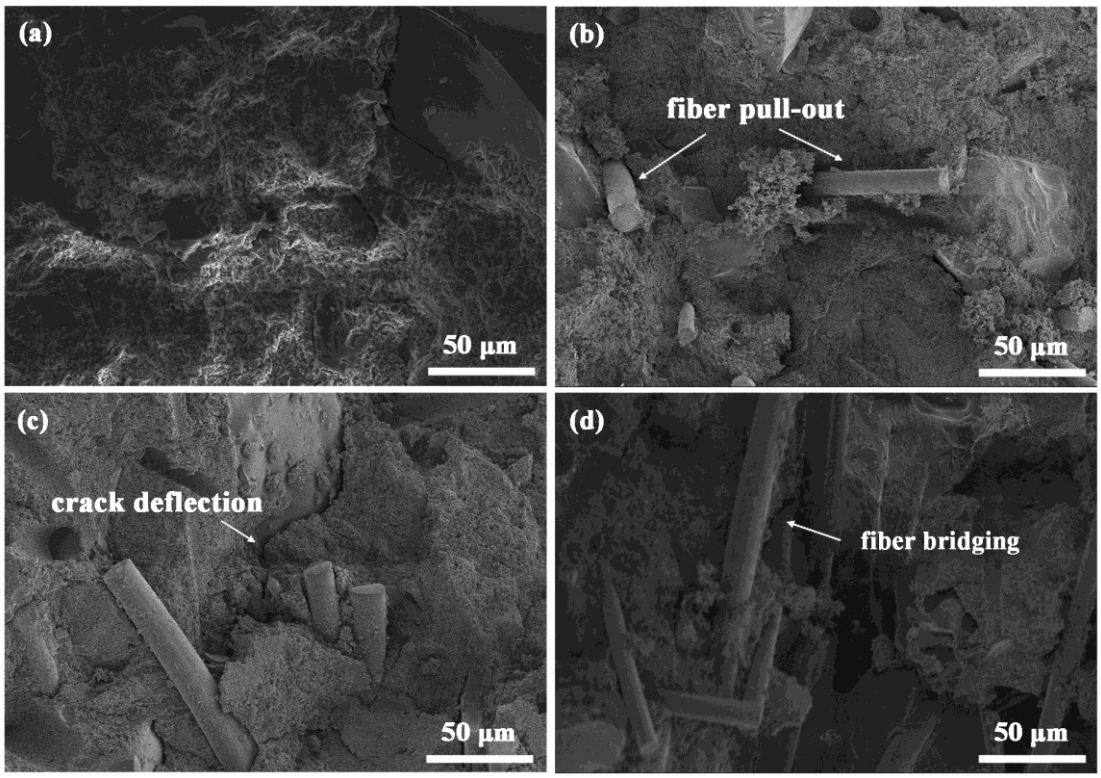

Figure 5: SEM images of crucible samples with different contents of mullite fibers: (a) 0 wt%, (b) 1 wt%, (c) 3 wt%, (d) 4 wt%

3.4. Thermal shock resistance

In order to evaluate the thermal shock resistance of the crucible, the crucible samples with 3 wt%

of mullite fibers are heated at 1300 ℃ for 0.5 h and then air cooled and quenched for 10 min. The residual room-temperature flexural strength and the strength retention rate compare to the initial strength of the crucible samples were measured after the sample underwent rapid heat and cooling cycles for 1, 2, 3 and 5 times, are shown in Fig.6. After once thermal shock, the room temperature flexural strength is 17.28 MPa, and the strength retention rate is 76.9%. After thermal shock for 5 times, the flexural strength of the sample decreases to 16.65 MPa, and the strength retention rate is 74.1%. Liu [34] tested the thermal shock resistance of alumina ceramics using the residual strength of the sample at a certain temperature difference. When the temperature difference is 700 ℃, the residual strength of the sample is about 45% of the initial strength. In Zhang's work [35], cordierite ceramics were heated to 900 ℃, and suffered water-cooled quenching to explore its thermal shock resistance. When the temperature difference is ΔT=450 ℃, the residual strength decreases to 1/3 of the initial strength. Ma [36] studied the thermal shock resistance of Al_2O_3-SiC-C refractory material by heating the sample to 1100 ℃ and water-cooled for 5 times, and the strength retention rate was less than 52%. In comparison, the high strength retention rate in this work indicates that the sample has good thermal shock stability, which can improve the service life of the crucible to withstand the temperature difference between high-temperature alloy melting and casting.

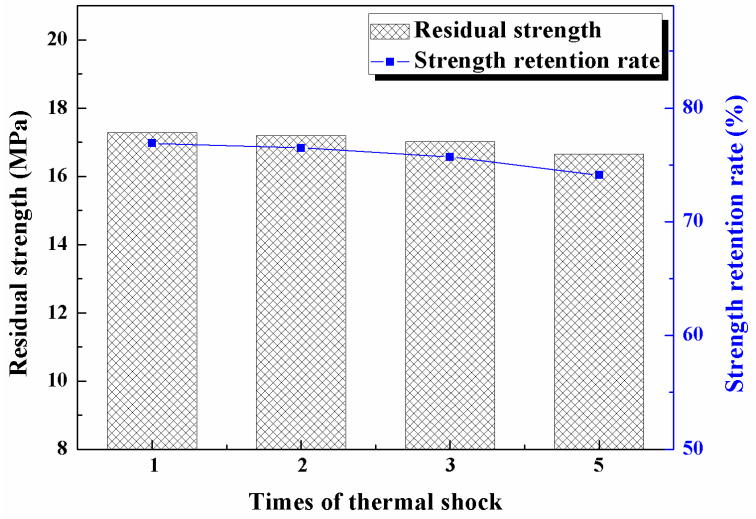

Figure 6: Residual strength and strength retention rate of samples with 3 wt% of mullite fibers.

4. Conclusions

In order to extend the service life for alumina-based crucible for superalloy smelting, alumina-based crucibles are prepared by slip casting, and mullite fibers are used as reinforcement phase. The effect of mullite fibers on the microstructure and property of the crucibles was studied. The appropriate content of mullite fibers are beneficial to the comprehensive performance of the crucibles. The reinforcement mechanism of mullite fibers includes crack deflection, fiber extraction, and fiber bridging, through which fibers hinder the initiation and propagation of cracks in ceramics. For the crucible samples with 3 wt% of mullite fibers, the values of flexure strength are 22.47 MPa and 19.14 MPa at room temperature and high-temperature, respectively. After thermal shock for 5 times, the residual room-temperature flexural strength is 16.65 MPa and the strength retention rate is 74.1%. It is confirmed that, the 3 wt% of mullite fibers improves the thermal shock resistance of the crucible, which is beneficial for extending the service life of the crucible for superalloy melting.

Acknowledgements

This work is supported by the Fundamental Research Funds for the Central Universities, CHD (300102312406, 300102313204).

References

[1] Kollova, A., Pauerova, K. Superalloys - characterization, usage and recycling, Manufacturing Technology, (2022) 22, 550-557.
[2] Lin, Y. C., Wu, X. Y., Chen, X. M., Chen, J., Wen, D. X., Zhang, J. L., Li, L. T. EBSD study of a hot deformed nickel-based superalloy, Journal of Alloys and Compounds, (2015) 640, 101-113.
[3] Bauer, A., Neumeier, S., Pyczak, F., Goken, M. Microstructure and creep strength of different gamma/gamma '-strengthened Co-base superalloy variants, Scripta Materialia, (2010) 63, 1197-1200.
[4] Henderson, M. B., Arrell, D., Larsson, R., Heobel, M., Marchant, G. Nickel based superalloy welding practices for industrial gas turbine applications, Science and Technology of Welding and Joining, (2004) 9, 13-21
[5] Zhang, C., Yang, B., Wang, Y., Tu, G. X. Preliminary research on a high thrust-to-weight ratio of double-sided composite impeller microturbine engine, International Journal of Aerospace Engineering, (2021) 9931701.
[6] Frenzel, J., Zhang, Z., Neuking, K., Eggeler, G. High quality vacuum induction melting of small quantities of NiTi shape memory alloys in graphite crucibles, Journal of Alloys and Compounds, (2004) 385, 214-223.
[7] Zhang, C., Wang, J., Zhang, H., Ding, B. Effects of Ni and Co on microstructure and characteristics of CuCr25 prepared by vacuum induction melting, Rare Metal Materials and Engineering, (2001) 30, 286-289.
[8] Sornlar, W., Choeycharoen, P., Wannagon, A. Characterization of alumina crucible made from aluminum industrial waste, Journal of the Australian Ceramic Society, (2019) 56(2), 1-9.
[9] Sembiringa, S., Simanjuntak, W., Situmeang, R., et al. Effect of alumina addition on the phase transformation and crystallisation properties of refractory cordierite prepared from amorphous rice husk silica, Journal of Asian Ceramic Societies, (2017) 5, 186-192.
[10] Fan, J. X., Fan, H. N., Song, Z., Guo, Y. J., Li, M. M., Li X., Qi, C. J., Xu, X. Q. Thermal-shock stable Al2O3 crucible for superalloy smelting through slip casting with particle gradation, Ceramics International, (2023) 49, 8762–8771.
[11] Li, Q. L., Zhang, H. R., Cui, Y. S., Yang, C. L., Gao, M., Li, J. P; Zhang, H. Behavior and Mechanism of High-Temperature Stability between Tial-Based Alloy and Y2O3-Al2O3 Composite Crucibles, Materials, (2018) 11, 1107.
[12] Jang, J., Lee, H. S., Lee, S. Stability of plasma-sprayed TiN and ZrN coatings on graphite for application to uranium-melting crucibles for pyroprocessing, Journal of Radioanalytical and Nuclear Chemistry, (2016) 310, 1173-1180.
[13] Fashu, S., Lototskyy, M., Davids, M. W., Pickering, L., Linkov, V., Tai, S., Renheng, T ., Xiao, F. M., Fursikov, P. V., Tarasov, B. P. A review on crucibles for induction melting of titanium alloys, Materials & Design, (2020) 186, 108295.
[14] Ma, L. M., Zhang, J. Z., Yue, GQ., Zhang, HR., Zhou, L., Zhang, H. Improvement and application of Y2O3 directional solidification crucible, Chinese Journal of Aeronautics, (2016) 29, 554-559.
[15] Tetsui, T., Kobayashi, T., Mori, T., Kishimoto, T. Harada, H., Evaluation of Yttria Applicability as a Crucible for Induction Melting of TiAl Alloy, Materials Transactions, (2010) 9, 1656-1662.
[16] Yuan, J. Service Effect of Quartz Crucible for Platinum Jewelry Casting, Special Casting & Nonferrous Alloys, (2018) 38, 25-28.
[17] Yu, J. K., Cui, C. W., Tian, X. Z., Wang, C., Wang, X. L., Dai, W. B. Fabrication of coarse grain yttria composite and its corrosion resistance to molten titanium, Journal of Ceramic Processing Research, (2017) 17, 1042-1045
[18] Alrobei, H., Hafiz, A., Malik, R. A. Design and manufacturing of lanthanum phosphate (LaPO4)-based crucible for high temperature applications, Journal of Ceramic Processing Research, (2021) 22, 499-503.
[19] Sembiring, S., Simanjuntak, W., Situmeang, R., Riyanto, A., Karo-Karo, P., Asian Ceram, J. Effect of alumina addition on the phase transformation and crystallisation properties of refractory cordierite prepared from amorphous rice husk silica, Journal of Asian Ceramic Societies, (2017) 5, 186-192.
[20] Lv, L., Lu, Y. J., Zhang, X. Y., Chen, Y. G., Huo, W. L., Liu, W., Yang, J. L. Preparation of low-shrinkage and high-performance alumina ceramics via incorporation of pre-sintered alumina powder based on Isobam gelcasting, Ceramics International, (2019) 45, 11654-11659.
[21] Golestani-fard, F., Mazaheri, M., Aminzare, M., Ebadzadeh, T. Microstructural evolution of a commercial ultrafine alumina powder densified by different methods, Journal of the European Ceramic Society, (2011) 31, 2593-2599.
[22] Wang, L. Y., An, L., Zhao, J., Shimai, S., Mao, X. J., Zhang, J., Liu, J., Wang, S. W. High-strength porous alumina

ceramics prepared from stable wet foams, Journal of Advanced Ceramics, (2021) 10, 852-859.
[23] Zhang, P., Zhou, F. S., Zhang, C., Yan, Z. M., Li, J. Y., Jin, H. Y., Zhang, H., Lu, J. Y. Charge trapping characteristics of alumina based ceramics, Ceramics International, (2018) 44, 12112-12117.
[24] Obikawa, T., Matsumura, T., Shirakashi, T., Usui, E. Wear characteristic of alumina coated and alumina ceramic tools, Journal of Materials Processing Technology, (1997) 63, 211-216.
[25] Liang, Y. Y., Chen, D. M., Tong, J. F. Compression Dynamic Performance of Bulletproof Alumina Ceramic, Rare Metal Materials and Engineering, (2013) 42, 956-959.
[26] Yang, R., Qi, Z., Gao, Y., Yang, J. H., Zhou, Y. R., Liu, H., Peng, L. M., Jiao, J. Effects of alumina sols on the sintering of alpha-alumina ceramics, Ceramics International, (2020) 43, 20865-20870.
[27] Lang, Y., Wang, C. A. Al2O3-fiber-reinforced porous YSZ ceramics with high mechanical strength, Ceramics International, (2014) 40, 10329-10335.
[28] Naslain, R. Design, preparation and properties of non-oxide CMCs for application in engines and nuclear reactors: an overview, Composites science and Technology, (2004) 64, 155-170.
[29] Wang, M., Liu, J., Du, H., et al. A SiC whisker reinforced high-temperature resistant phosphate adhesive for bonding carbon/carbon composites, Journal of Alloys and Compounds, (2015) 633, 145-152.
[30] Li, L. Damage development in fiber-reinforced ceramic-matrix composites under cyclic fatigue loading using hysteresis loops at room and elevated temperatures, International Journal of Fracture, (2016) 199, 39-58.
[31] Reinders, L., Pfeifer, S., Kroener, S., Stolpmann, H., Renfftlen, A., Greiler, L. C., Clauss, B., Buchmeiser, M. R. Development of mullite fibers and novel zirconia-toughened mullite fibers for high temperature applications, Journal of the European Ceramic Society, (2021) 41, 3570-3580.
[32] Dong, X., Liu, J. Q., Li, X. T., Zhang, X. J., Xue, Y. J., Liu, J. C., Guo, A. R., Electrospun mullite nanofibers derived from diphasic mullite sol, Journal of the American Ceramic Society, (2017)100, 3425-3433.
[33] Niu, S., Xu, X., Li, X., et al. Microstructure evolution and properties of silica-based ceramic cores reinforced by mullite fibers, Journal of Alloys and Compounds, (2020) 829, 154494.
[34] Liu, C., Cai, C., Xie, J., et al. Effect of surface brittle-to-ductile transition on high-temperature thermal shock resistance of Al2O3 ceramics, Ceramics International, (2022) 48(14), 20627-20638.
[35] Zhang, L., Olhero, S., Ferreira, J. M. F. Thermo-mechanical and high-temperature dielectric properties of cordierite-mullite-alumina ceramics, Ceramics International, (2016) 42(15), 16897-16905.
[36] Ma, J., Zhao, H., Yu, J., et al. The critical role of aggregate microstructure in thermal shock resistance and slag resistance of Al2O3-SiC-C castable, Ceramics International, (2022) 48(8), 11644-11653.